

Co-doped TiO₂ Anatase – An Exciting New Magnetic Semiconductor for Spintronics*

S.A Chambers, A.C. Tuan¹, T. Droubay, S. Thevuthasan, D.E. McCready, S. Lea, C. Wang, J. Young, S. Shutthanandan, C.F. Windisch, Jr. (PNNL)

R.F.C. Farrow, R.F. Marks, J.-U.Thiele, L. Folks, M.G. Samant (IBM Almaden Research Center, San Jose, CA)

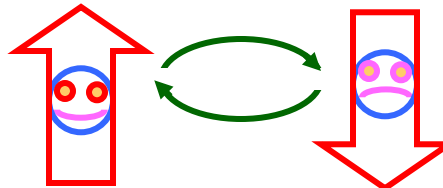
D. Schmidt, M.A. Olmstead (Department of Physics, University of Washington, Seattle, WA)

1 – Also at Department of Chemical Engineering, University Of Washington, Seattle, WA

***Work at PNNL supported by PNNL LDRD Nanoscience and Technology Initiative & DOE BES Materials Science**

Background

What is “*sp[↑]intronics*”?



Def -- using the spin of quantum mechanical particles to carry signals and process information in new ways

In contrast – electronics → using the charge of electrons and holes to carry signals and process information

Why? – to gain new functionality, and to minimize size and power dissipation

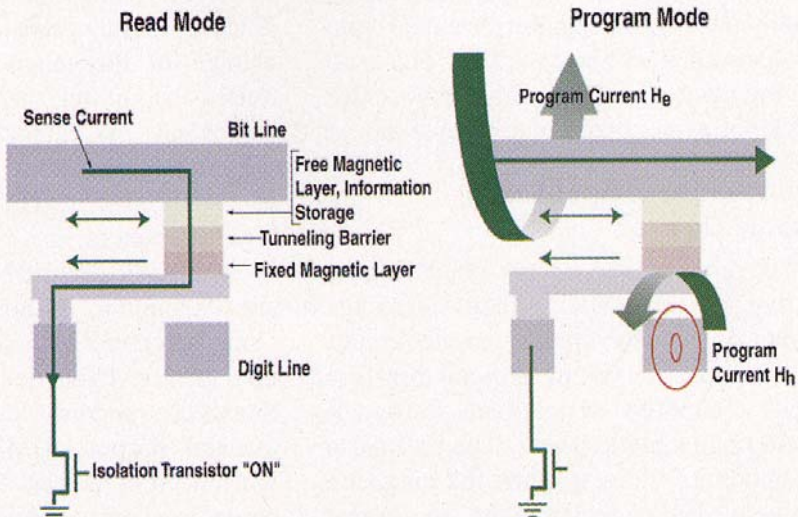
- Examples* –
- (1) magnetoresistive random access memory (MRAM) → nonvolatile memory
 - (2) spin-based devices (LEDs, RTDs, FETs, optical switches)
→ higher speed and new functionality
 - (3) quantum bit based devices → quantum computation

MRAM

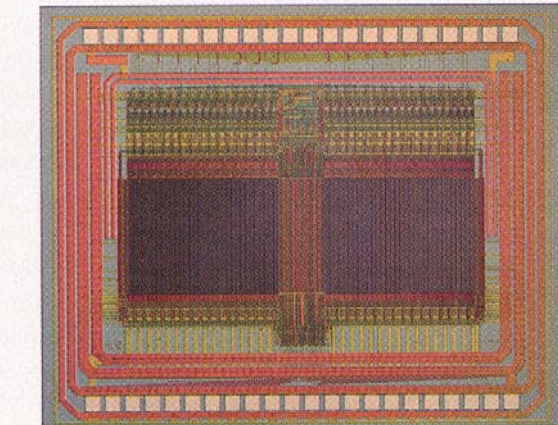
Based on magnetic tunnel junctions (MTJs)



C) 1T1MTJ MRAM Cell (Motorola)



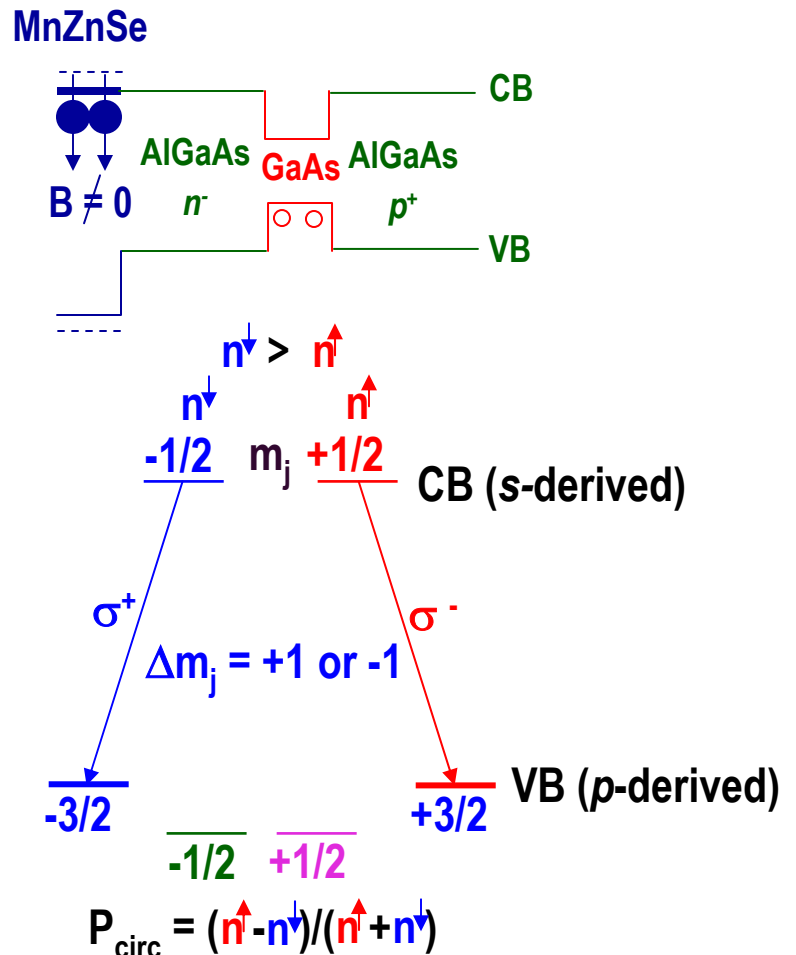
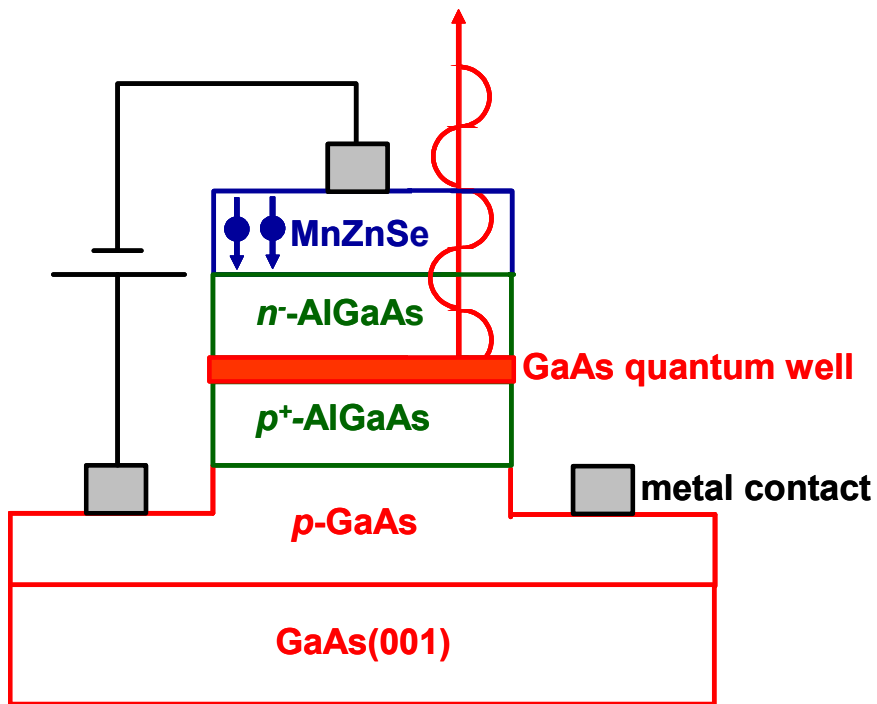
D) 256 Kb MRAM chip



$$R_p < R_{ap}$$
$$\Delta R/R = 20 - 50\%$$
$$\text{Sat field} = 10 - 30 \text{ Oe}$$

S. Wolf et al., Science 294, 1488 (2001)

spin LED



>50% spin injection efficiency – at a few degrees K

Application – photonic encryption (any form of tampering will destroy the light polarization)

Quantum Computation

- Based on the concept of quantum bits (“qubits”)
- 1 qubit = 1 spin

1 spin ($s=1/2$): $\psi(1) = c_1|\alpha(1)\rangle + c_2|\beta(1)\rangle$
 $\rightarrow 2 \text{ complex numbers}$

2 spins ($s=1/2$): $\psi(1,2) = c_1|\alpha(1)\rangle|\alpha(2)\rangle + c_2|\alpha(1)\rangle|\beta(2)\rangle$
 $+ c_3|\beta(1)\rangle|\alpha(2)\rangle + c_4|\beta(1)\rangle|\beta(2)\rangle$
 $\rightarrow 4 \text{ complex numbers}$

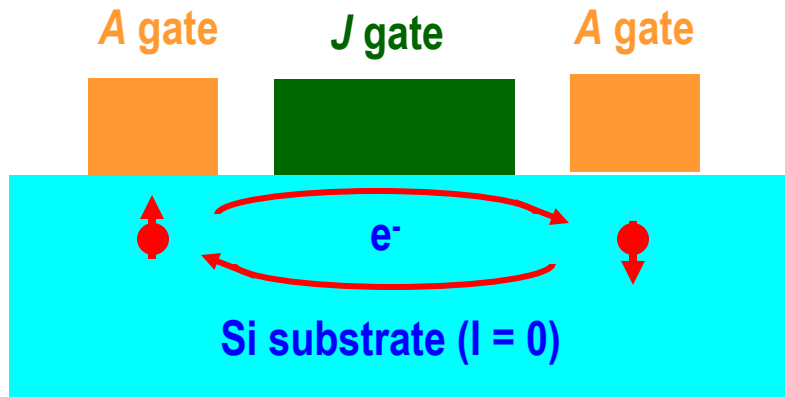
3 spins ($s=1/2$): $\psi(1,2,3) = c_1|\alpha(1)\rangle|\alpha(2)\rangle|\alpha(3)\rangle + c_2|\alpha(1)\rangle|\alpha(2)\rangle|\beta(3)\rangle$
 $+ c_3|\alpha(1)\rangle|\beta(2)\rangle|\alpha(3)\rangle + c_4|\beta(1)\rangle|\alpha(2)\rangle|\alpha(3)\rangle$
 $+ c_5|\beta(1)\rangle|\beta(2)\rangle|\alpha(3)\rangle + c_6|\beta(1)\rangle|\alpha(2)\rangle|\beta(3)\rangle$
 $+ c_7|\alpha(1)\rangle|\beta(2)\rangle|\beta(3)\rangle + c_8|\beta(1)\rangle|\beta(2)\rangle|\beta(3)\rangle$
 $\rightarrow 8 \text{ complex numbers}$

N spins $\rightarrow 2^N \text{ complex numbers}$ (no entanglement)

34 independent qubits $\rightarrow 10$ Gbytes of RAM!

Quantum Computation – A Device Concept

Use the nuclear spin of P dopants (spin $\frac{1}{2}$) in Si (zero spin)



● - ^{31}P (shallow donor – $I = 1/2$)

B. Kane, Nature 393, 133 (1998)

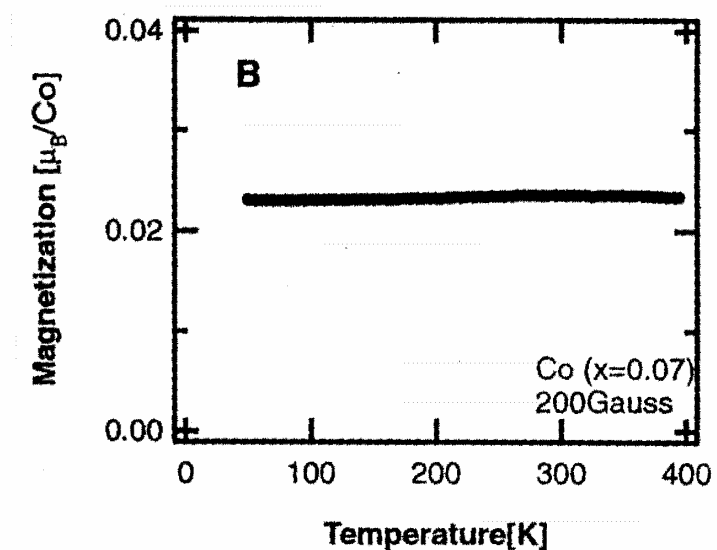
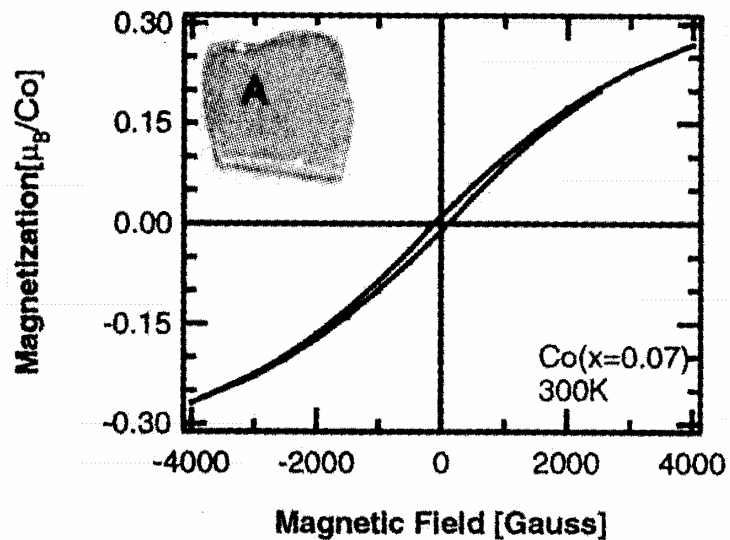
- *A* gates control hyperfine interaction (and magnetic resonance frequency) at individual ^{31}P nuclei
- *J* gates control electron density (and electron mediated coupling) between ^{31}P nuclei
- ^{31}P nuclear spin state “read” by tuning *A* gate voltages so 2 e^- from 2 ^{31}P donors occupy a single D⁻ state, which has a singlet ground state, and can be detected via capacitance measurements

A critical materials need...spin injectors for semiconductor heterostructures that work at RT

- Diluted magnetic semiconductors (DMS) of interest as efficient *electrical* spin injectors for semiconductor heterostructures
 - Conductivity matching very important – Schmidt *et al.* PRB 62, R4790 (2000)
- Most work thus far centered on Mn-doped II-VIs for spin injection into III-Vs (Curie temps. < ~110K)
 - Fiederling *et al.* -- Nature 402, 787 (1999)
 - Jonker *et al.* – PRB 62, 8180 (2000)
- Very recent work on Mn_xGe_{1-x} grown on GaAs (Curie temp. < ~116K)
 - Park *et al.* – Science 295, 651 (2002)
- *Nothing yet for Si!* One possibility we have suggested.....
 - Co-doped TiO₂ (anatase)
 - Promising based on PLD (Matsumoto *et al.* -- Science 291, 854 (2001))
- Our approach – grow Co-doped TiO₂ using OPA-MBE
 - Greater control & better quality material

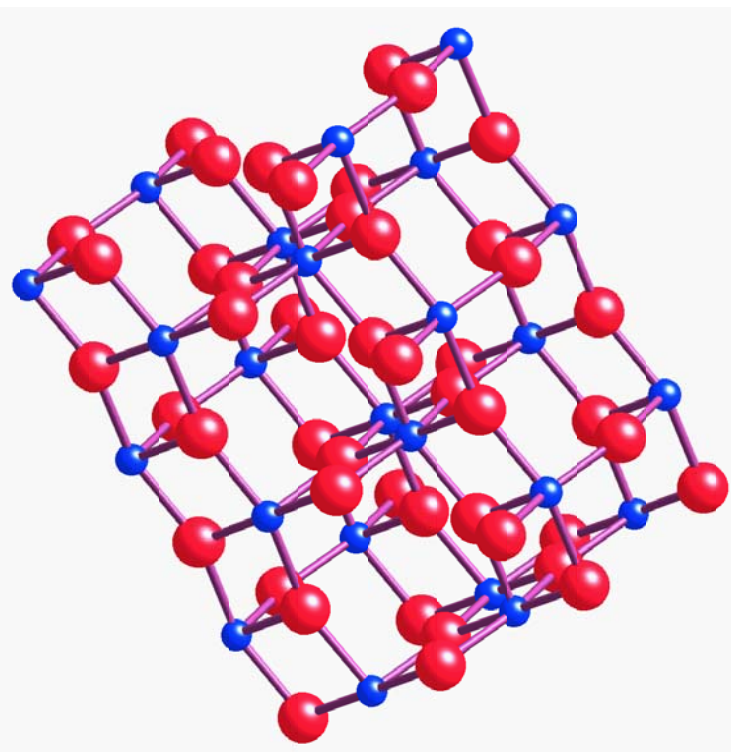
Matsumoto et al. -- Science 291, 854 (2001)

- PLD of $\text{Co}_x\text{Ti}_{1-x}\text{O}_2$ ($x \leq \sim 0.08$) on:
 1. SrTiO_3 ($\Delta a/a = -3.1\%$)
 2. $\text{LaAlO}_3(001)$ ($\Delta a/a = -0.26\%$)
- Targets: TiO_2 and $\text{Co}_{0.5}\text{Ti}_{0.5}\text{O}_2$
- $P = 10^{-5}$ to 10^{-6} Torr O_2
- $T_{\text{sub}} = 750\text{C}$
- Very low saturation magnetization ($\sim 0.3 \mu_B/\text{Co}$)
- Very low remanence ($\sim 3\%$)
- Very high saturation field ($> 4\text{KG}$)
→ domain-pinning defects
- But.....Curie temperature $> 400\text{K}$



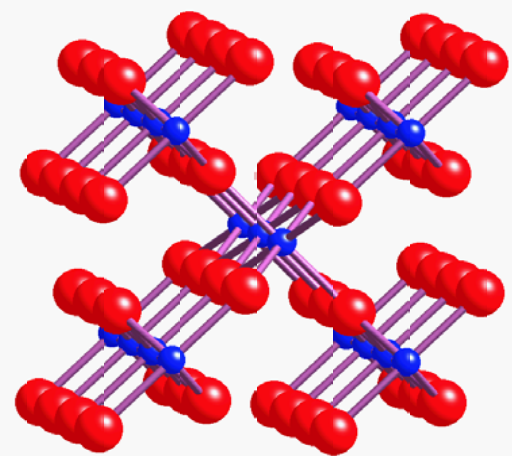
Anatase vs. Rutile

anatase



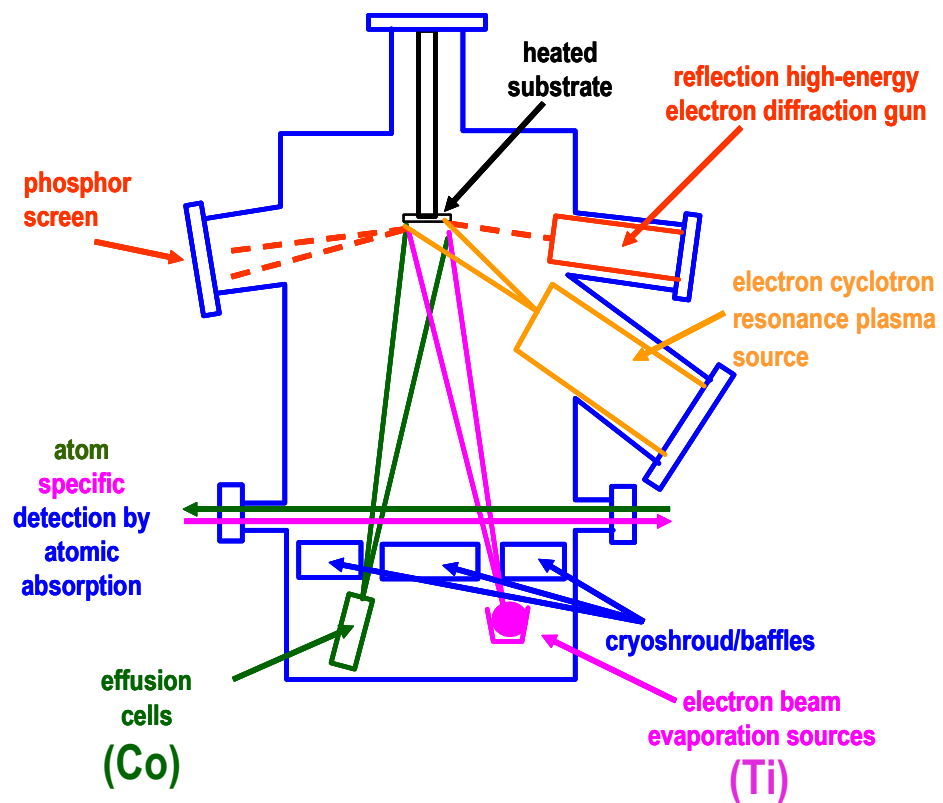
- $I4_1/amd$ space group
- $a = 0.379 \text{ nm}$; $c = 0.952 \text{ nm}$
- Highly distorted octahedral coordination
- Ti – O bond lengths = 0.198 nm (4x); 0.195 nm (2x)

rutile



- $P4_2/mnm$ space group
- $a = 0.459 \text{ nm}$; $c = 0.296 \text{ nm}$
- Octahedral coordination
- Ti – O bond lengths = 0.195 nm (4x); 0.198 nm (2x)

OPA-MBE Growth Conditions

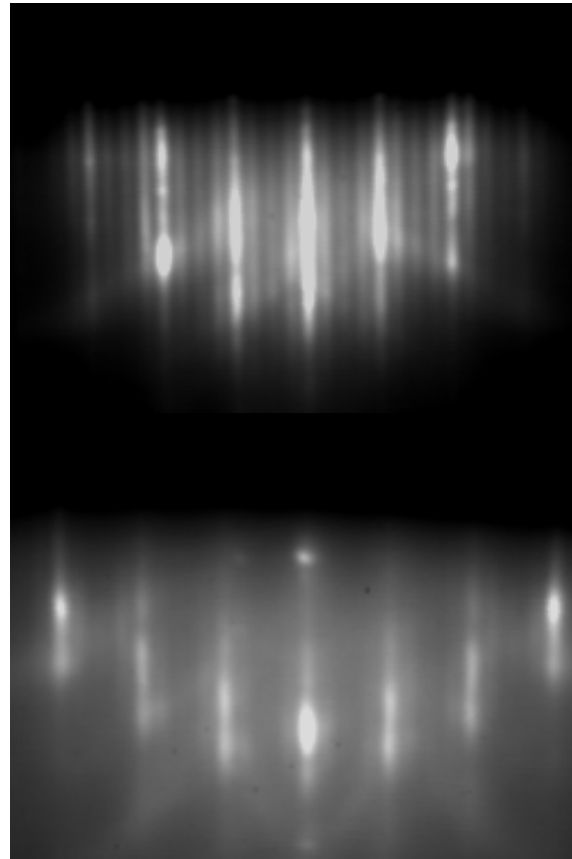


- $T_{\text{sub}} = 300\text{C} \rightarrow 750\text{C}$ (epi for $\sim 550\text{C}$)
- Ti flux (e beam evap – AA monitored & controlled) = $0.006 - 0.020 \text{ nm/sec}$
→ anatase growth rate = $0.05 - 0.17 \text{ ML/sec}$
- Co flux (hi T K cell) = $0 \rightarrow 0.0001 \text{ nm/sec}$
- $P_{\text{O}_2} = 1.0 - 2.0 \times 10^{-5} \text{ Torr}$
- Plasma power = 220W
- Same conditions produces TiO_2 rutile on $\text{TiO}_2(110)$
→ anatase grows by virtue of substrate stabilization

Surface Crystallography – $\text{TiO}_2/\text{LaAlO}_3(001)$

$T_{\text{sub}} = 650^\circ\text{C}$

growth rate =
0.003 nm/sec
(20 nm)



$T_{\text{sub}} = 550^\circ\text{C}$

growth rate =
0.037 nm/sec
(50 nm)



growth rate =
0.011 nm/sec
(20 nm)

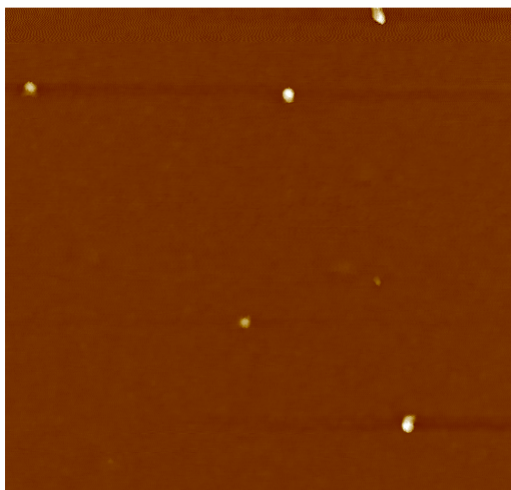
growth rate =
0.037 nm/sec
(50 nm)

Surface Morphology -- $\text{TiO}_2/\text{LaAlO}_3(001)$

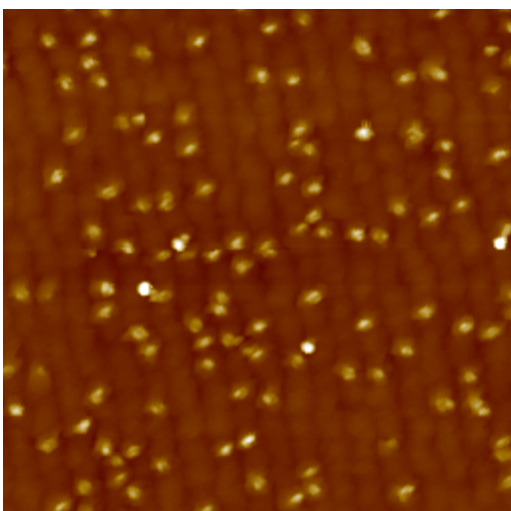
$T_{\text{sub}} = 650^\circ\text{C}$

$T_{\text{sub}} = 550^\circ\text{C}$

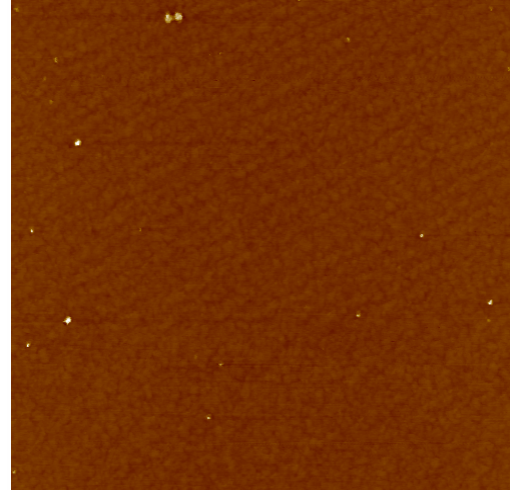
growth rate =
0.003 nm/sec
(20 nm)
 $\Delta z = 0 \rightarrow 50$ nm



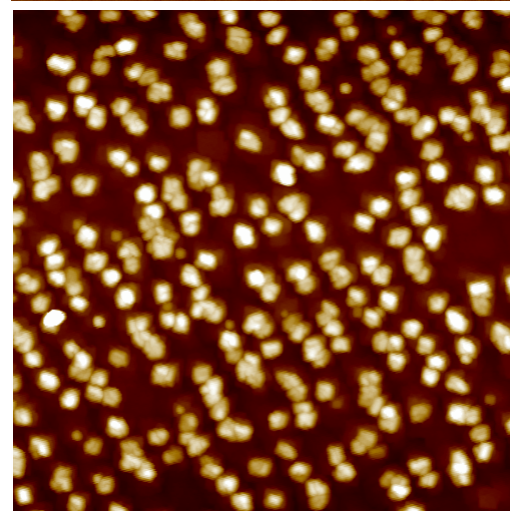
growth rate =
0.037 nm/sec
(50 nm)
 $\Delta z = 0 \rightarrow 50$ nm



growth rate =
0.011 nm/sec
(20 nm)
 $\Delta z = 0 \rightarrow 20$ nm

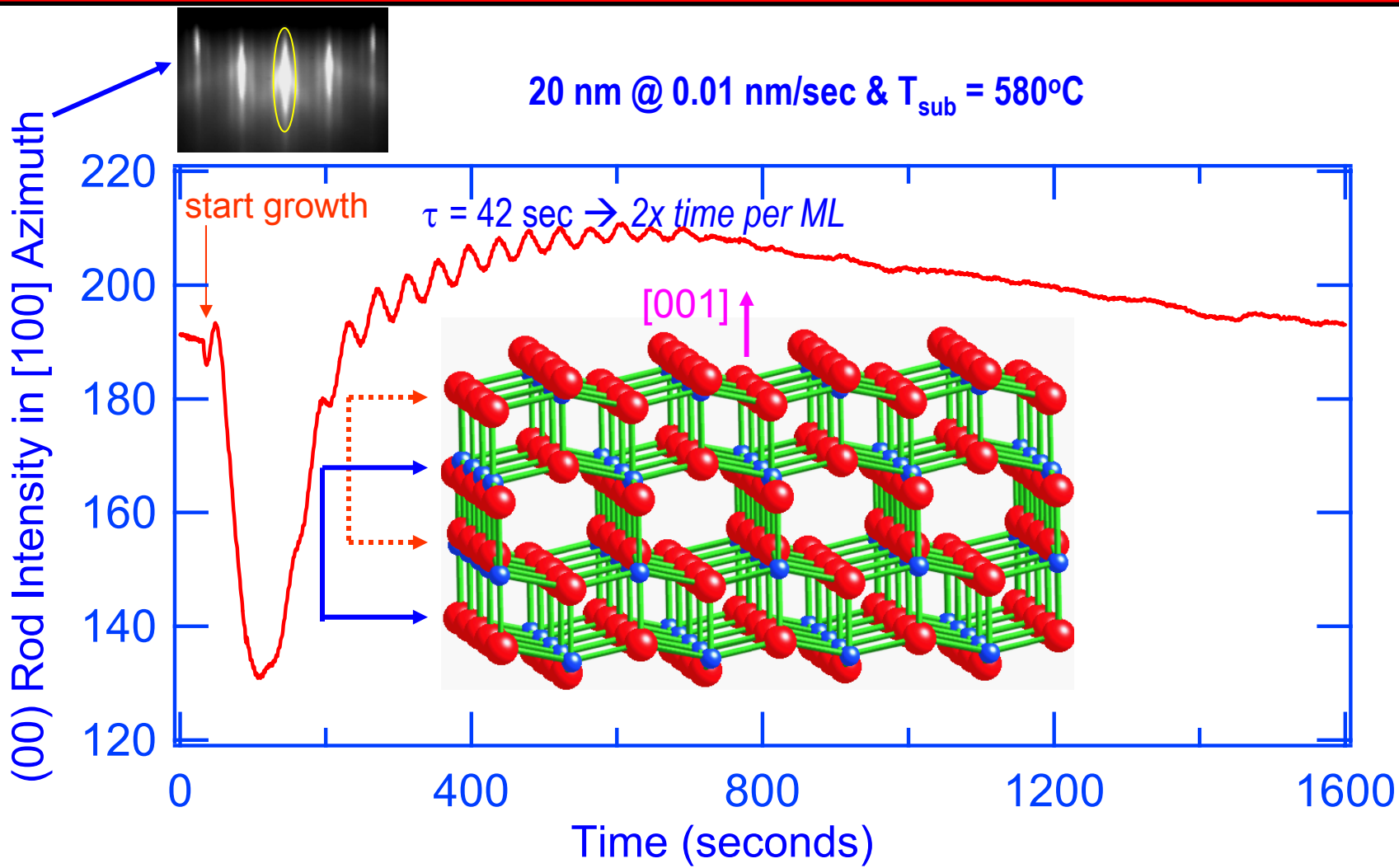


growth rate =
0.037 nm/sec
(50 nm)
 $\Delta z = 0 \rightarrow 50$ nm



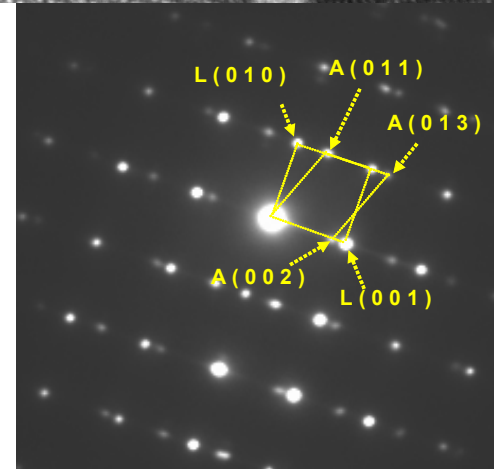
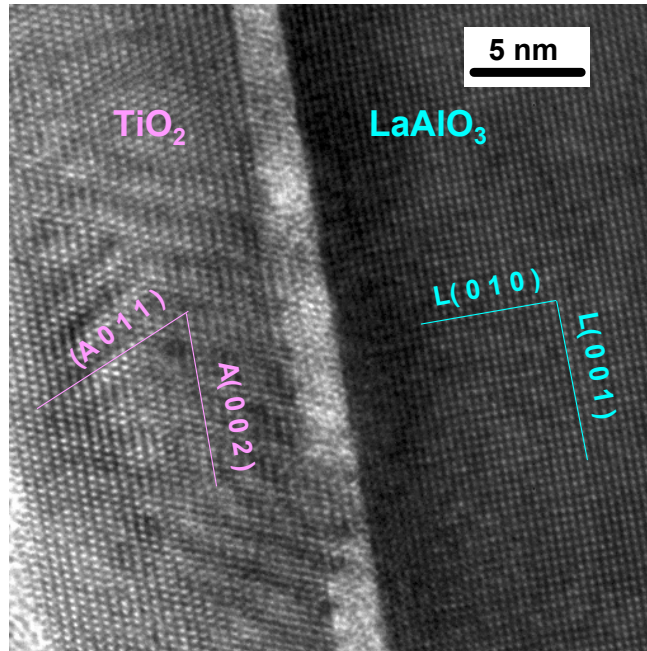
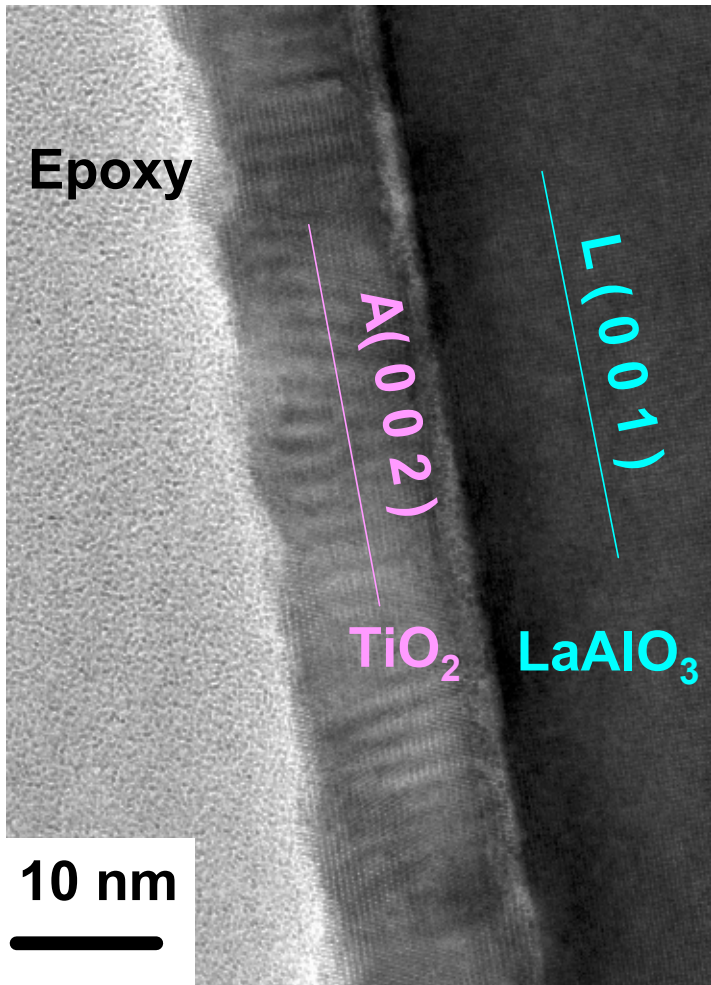
2 $\mu\text{m} \times 2 \mu\text{m}$

Layer-by-Layer Growth -- $\text{TiO}_2/\text{LaAlO}_3(001)$



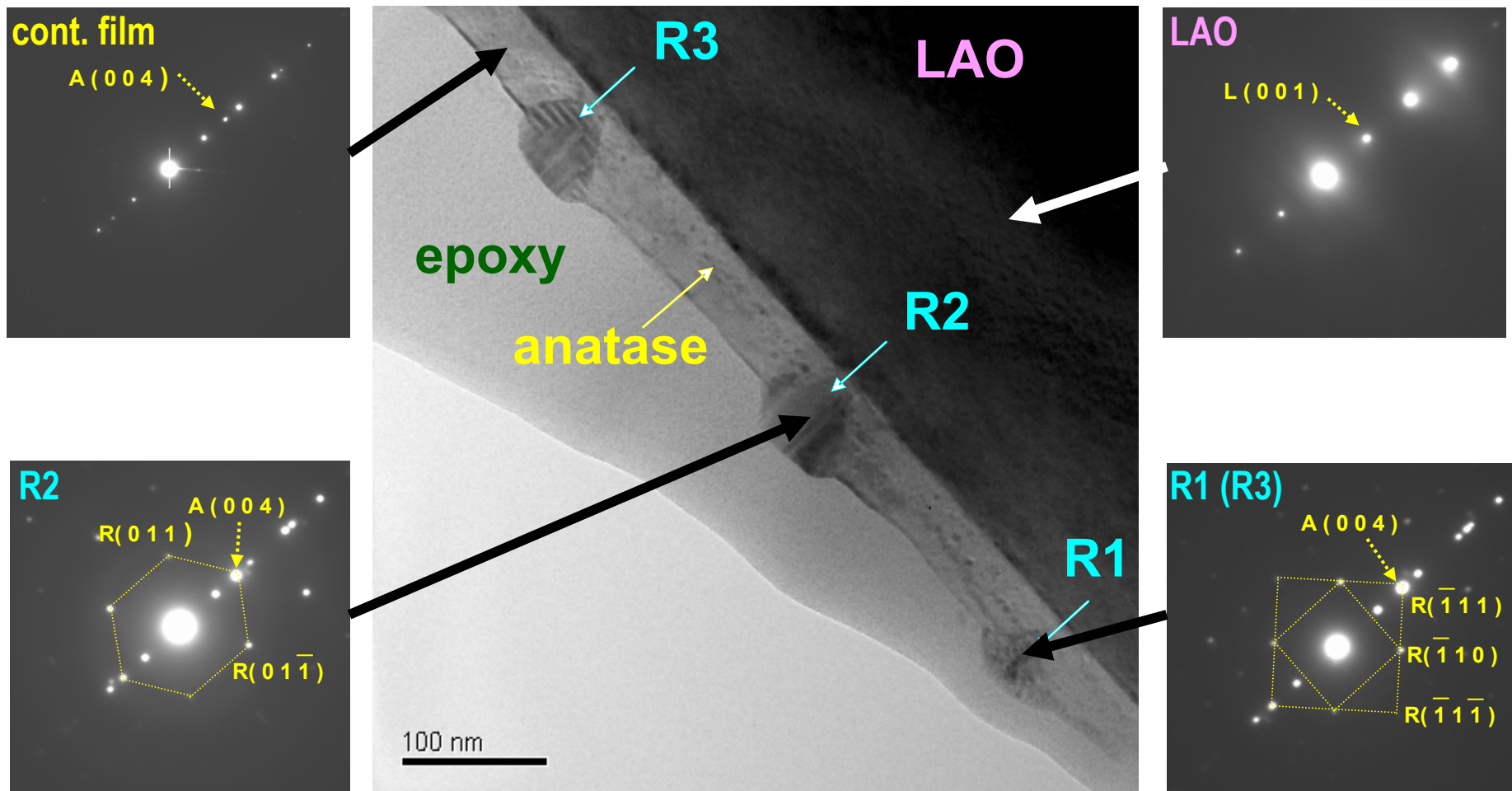
Microstructure -- $\text{TiO}_2/\text{LaAlO}_3(001)$

$r = 0.01 \text{ nm/sec (550}^{\circ}\text{C)}$



Microstructure -- $\text{TiO}_2/\text{LaAlO}_3(001)$

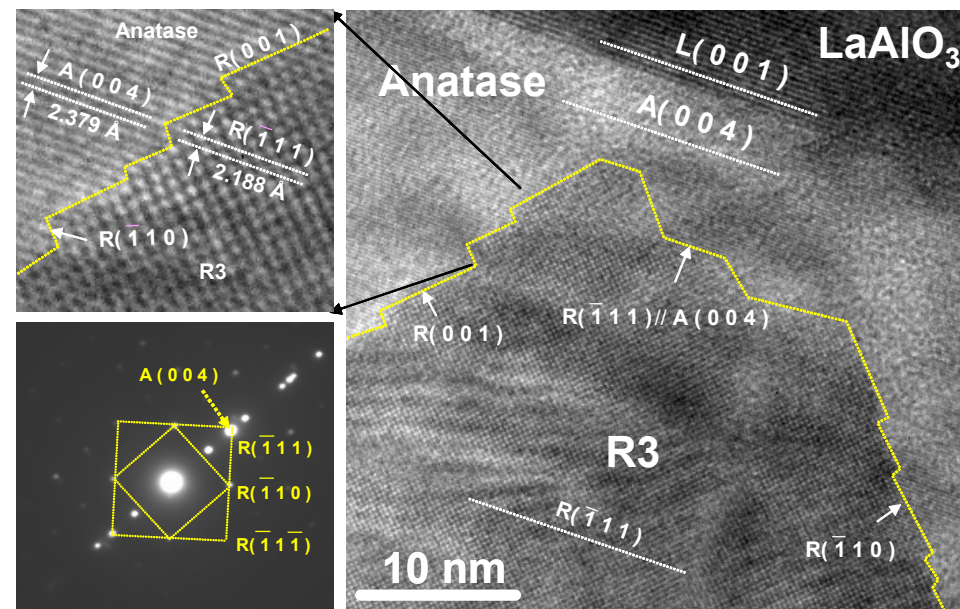
$r = 0.04 \text{ nm/sec (} 650^\circ\text{C})$



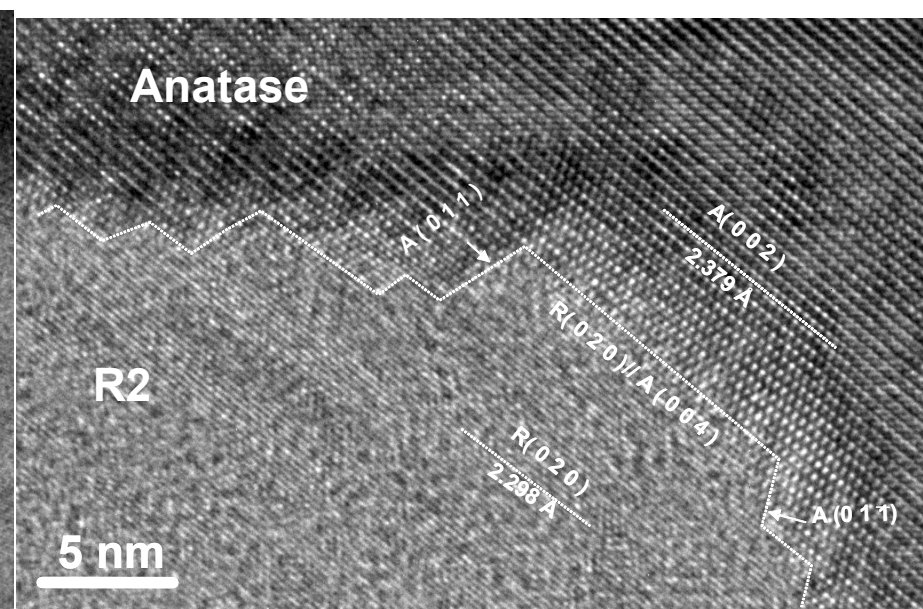
R2 & R3/anatase Interfaces in $\text{TiO}_2/\text{LaAlO}_3(001)$

$r = 0.04 \text{ nm/sec (} 650^\circ\text{C})$

R3/anatase



R2/anatase



Surface Crystallography -- $\text{Co}_x\text{Ti}_{1-x}\text{O}_2/\text{LaAlO}_3(001)$

[100]

$x = 0.01$
(20 nm)

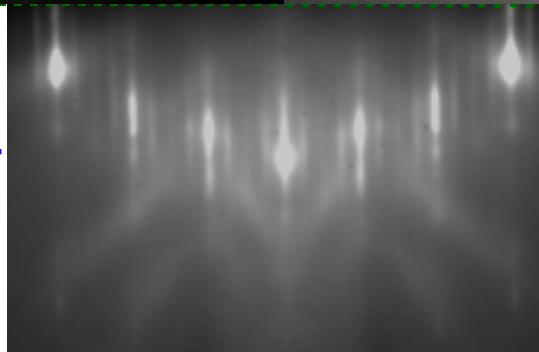
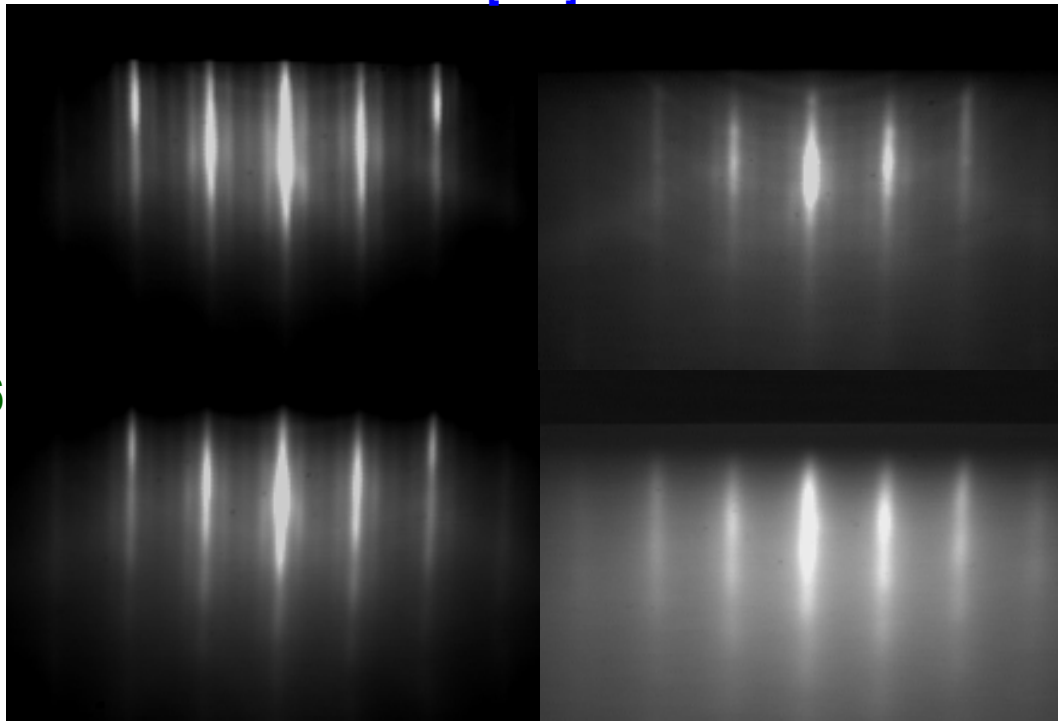
$x = 0.06$
(20 nm)

slow growth
(0.01 nm/sec)
↑
fast growth
(0.04 nm/sec)
↓
(50 nm)

$x = 0.03$
(20 nm)

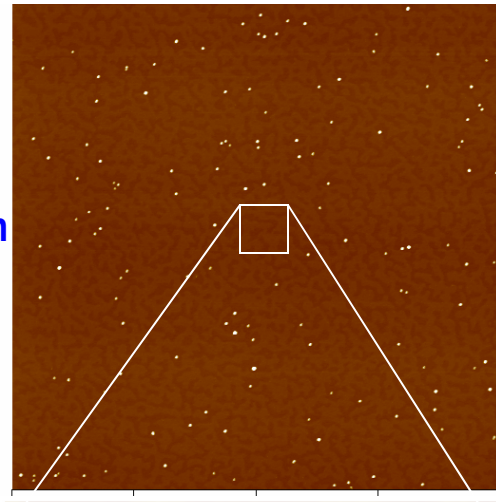
$x = 0.1$
(20 nm)

$x = 0.04$
(50 nm)



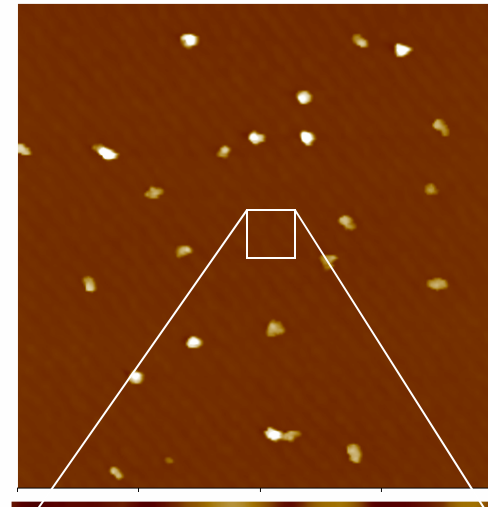
Surface Morphology – $\text{Co}_x\text{Ti}_{1-x}\text{O}_2/\text{LaAlO}_3(001)$

$r = 0.01 \text{ nm/sec}$, $x = 0.06$, 21 nm



1μm x 1μm x 10nm

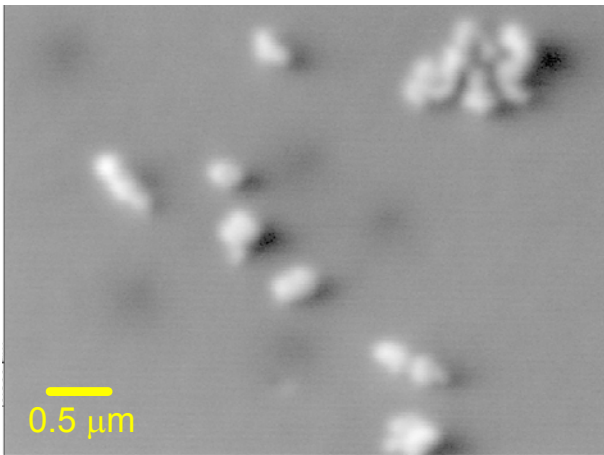
$r = 0.04 \text{ nm/sec}$, $x = 0.04$, 100 nm



1μm x 1μm x 10nm

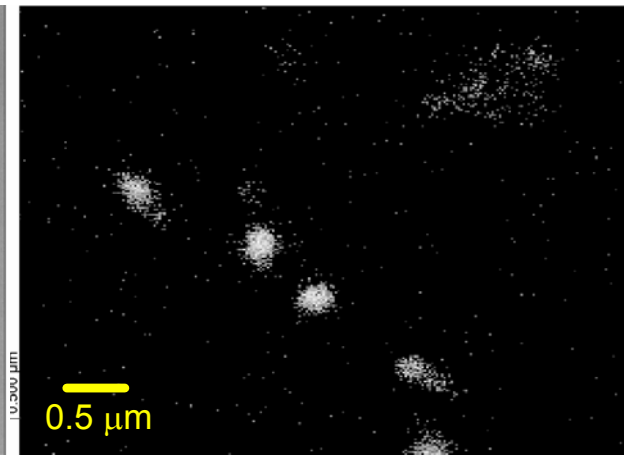
Co Distribution at Different Growth Rates

SEM image



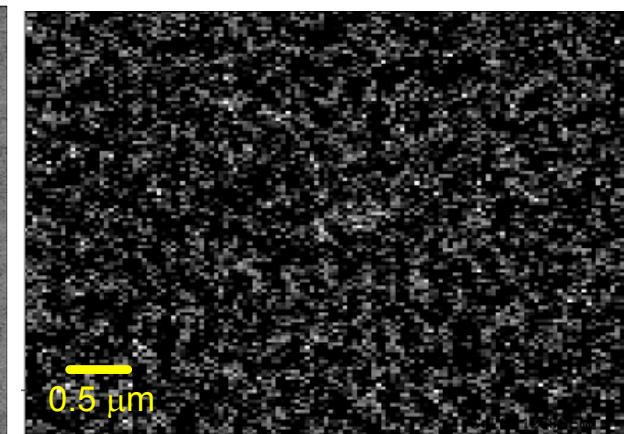
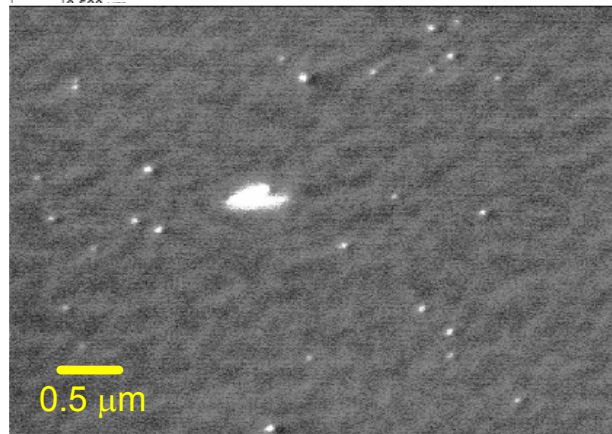
100 nm, $x = 0.04$
 $r = 0.04 \text{ nm/sec}$
 $T_{\text{sub}} = 650^\circ\text{C}$

Co LMM map

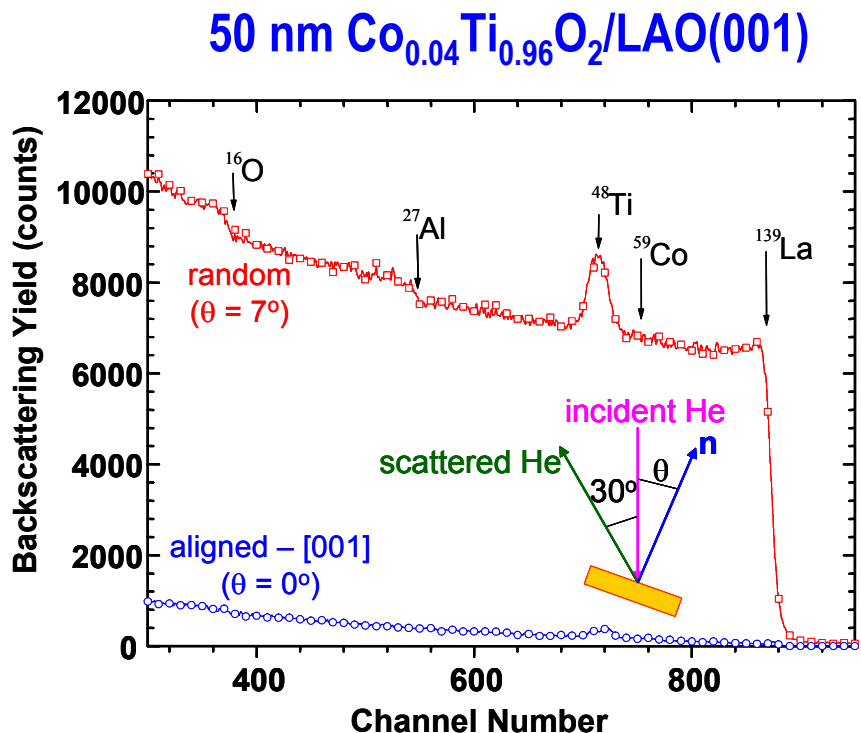


On terraces,
 $x = \sim 0$
On islands,
 $x = \sim 0.25$

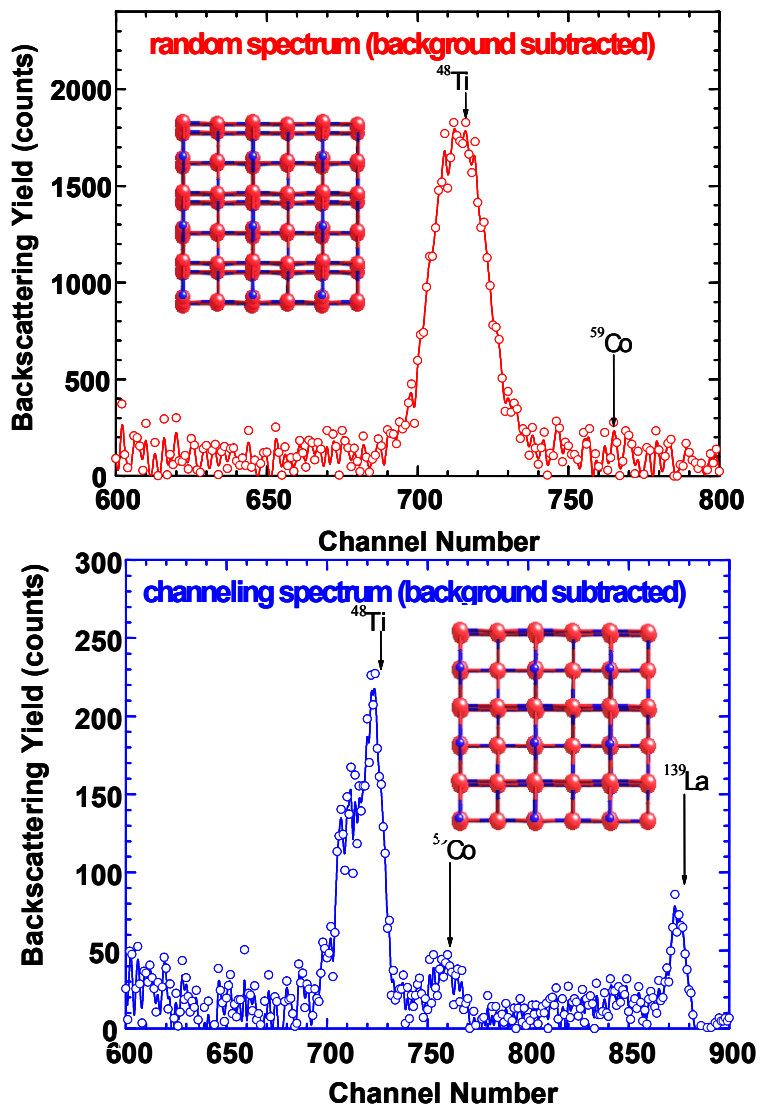
21 nm, $x = 0.06$
 $r = 0.01 \text{ nm/sec}$
 $T_{\text{sub}} = 550^\circ\text{C}$



Co Substitution at Ti Lattice Sites -- LAO

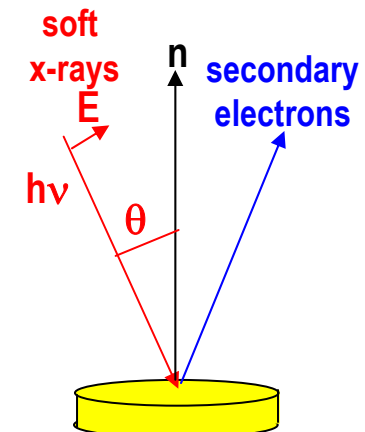
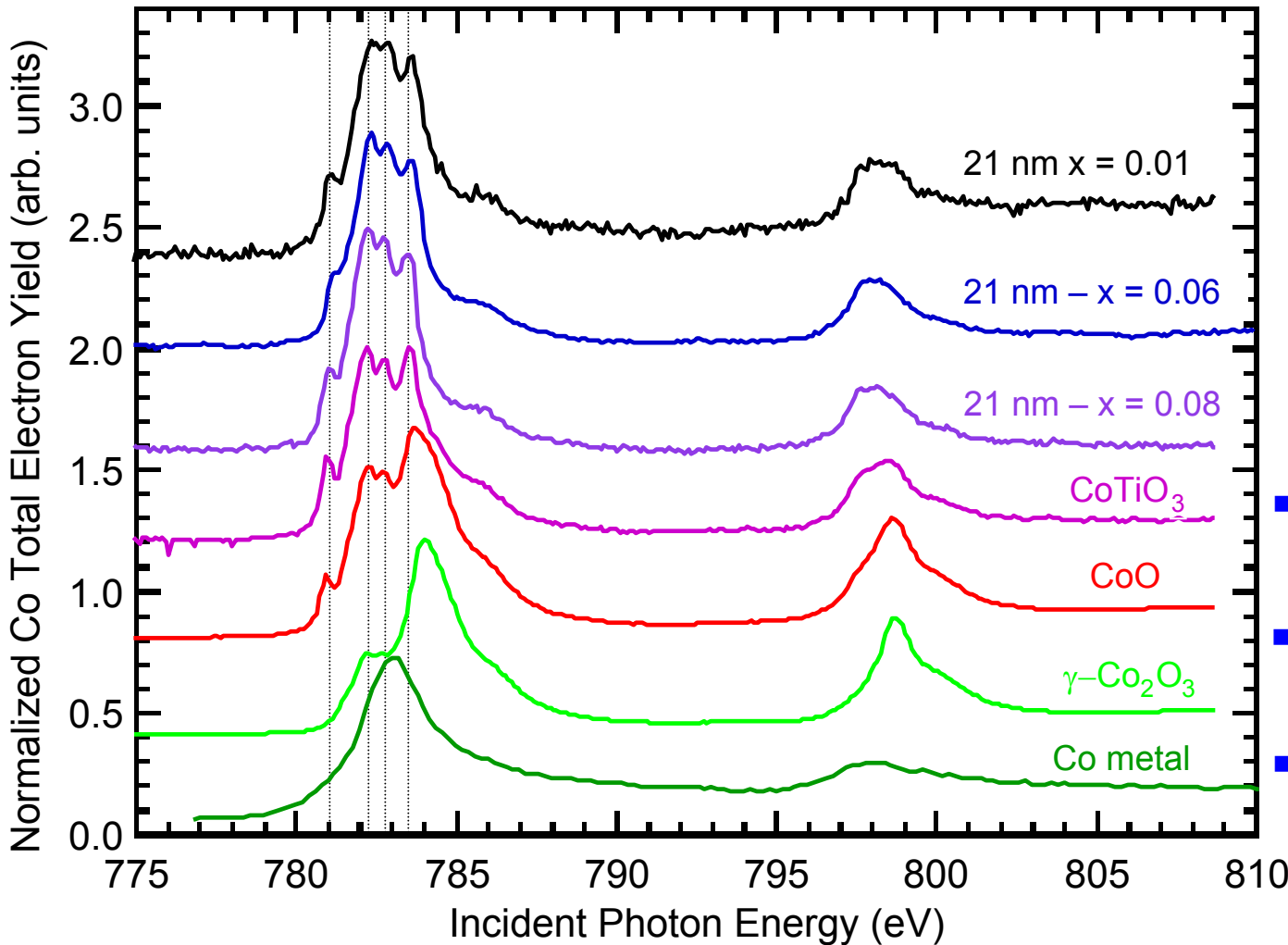


$$\chi_{\min} = \sim 10\% \text{ (Ti)} \text{ & } \sim 20\% \text{ (Co)}$$



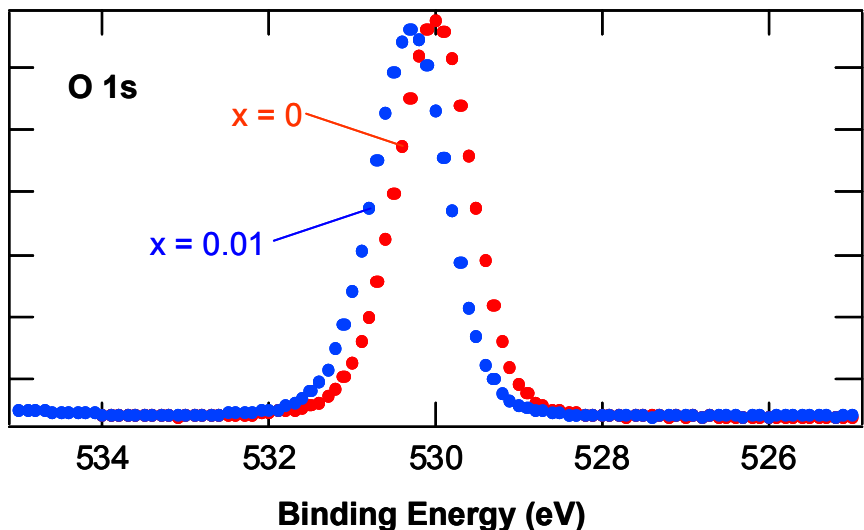
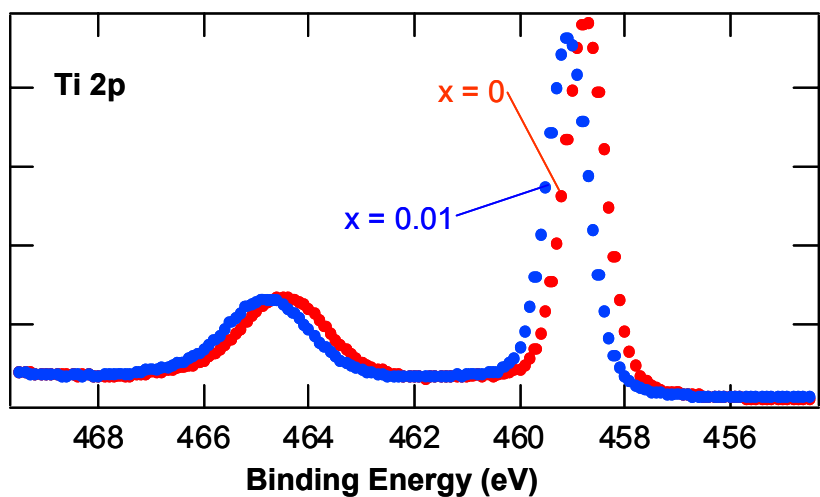
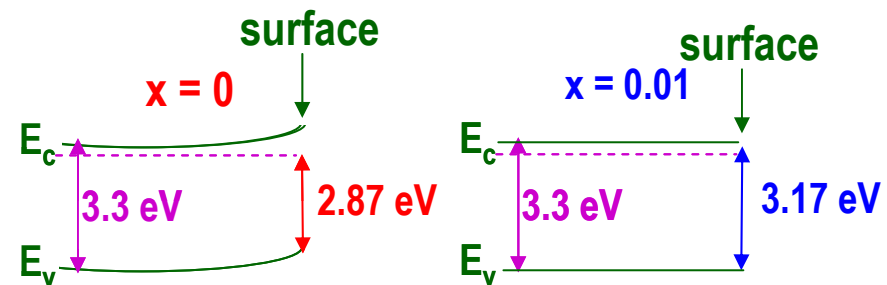
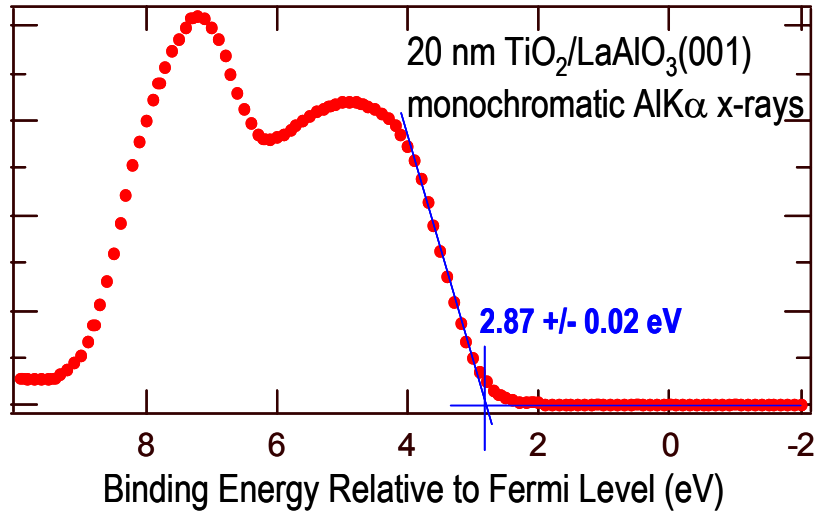
Co Charge State and Local Coordination

Co L-edge x-ray absorption spectroscopy – LBNL Advanced Light Source



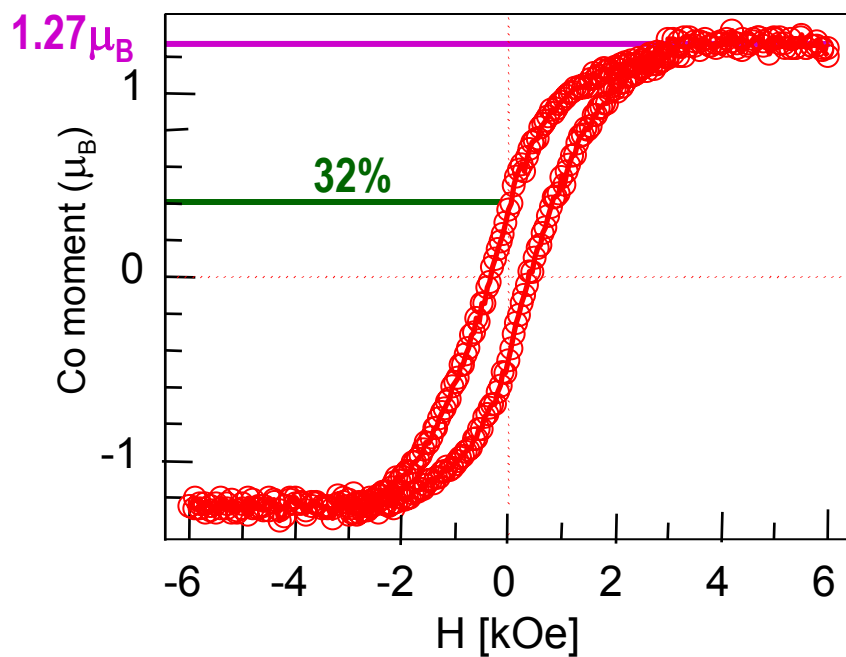
- Co in +2 formal oxidation state
- Co local structure like that in CoTiO_3
- Ferromagnetism not due to Co metal precipitates

$\text{Co}_x\text{Ti}_{1-x}\text{O}_2$ films are *n*-type semiconductors despite no intentional doping!



Magnetic Properties at Room Temperature - STO

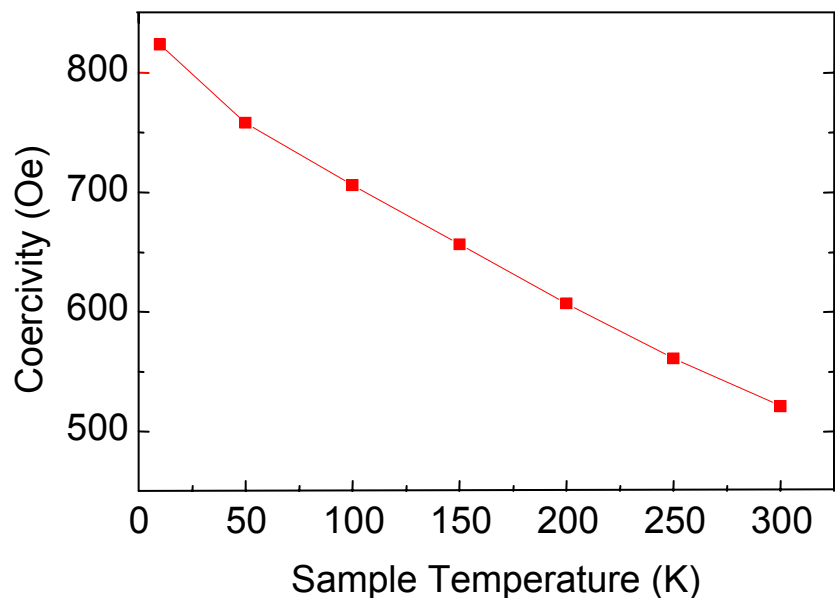
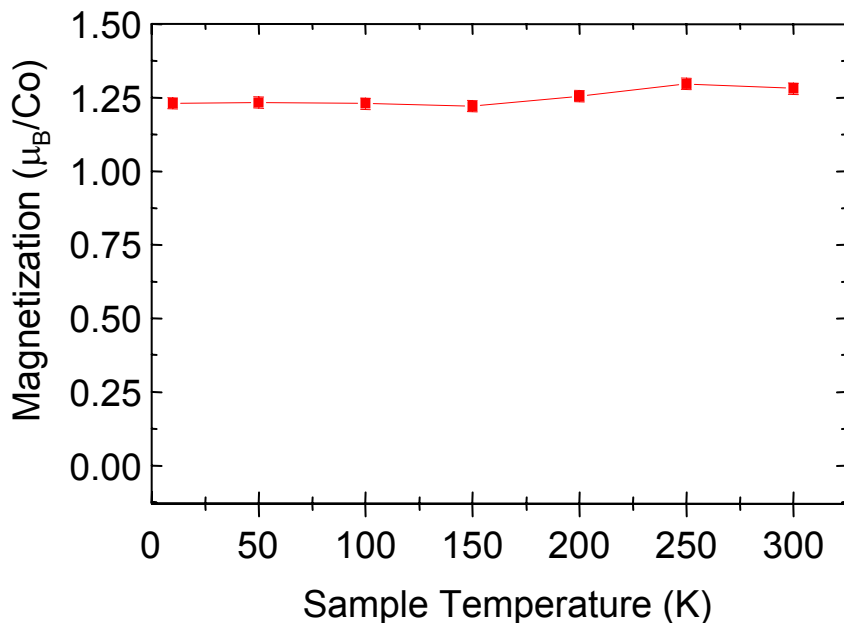
100 nm $\text{Co}_{0.02}\text{Ti}_{0.98}\text{O}_{1.98}/\text{SrTiO}_3(001)$ -- vibrating sample magnetometry



- Moment per Co(II) = $1.27\mu_B$ at saturation ($\sim 5x$ larger than PLD film moment)
- Remanence = 32% ($\sim 10x$ larger than PLD film remanence)

Magnetic Properties vs. Temperature - STO

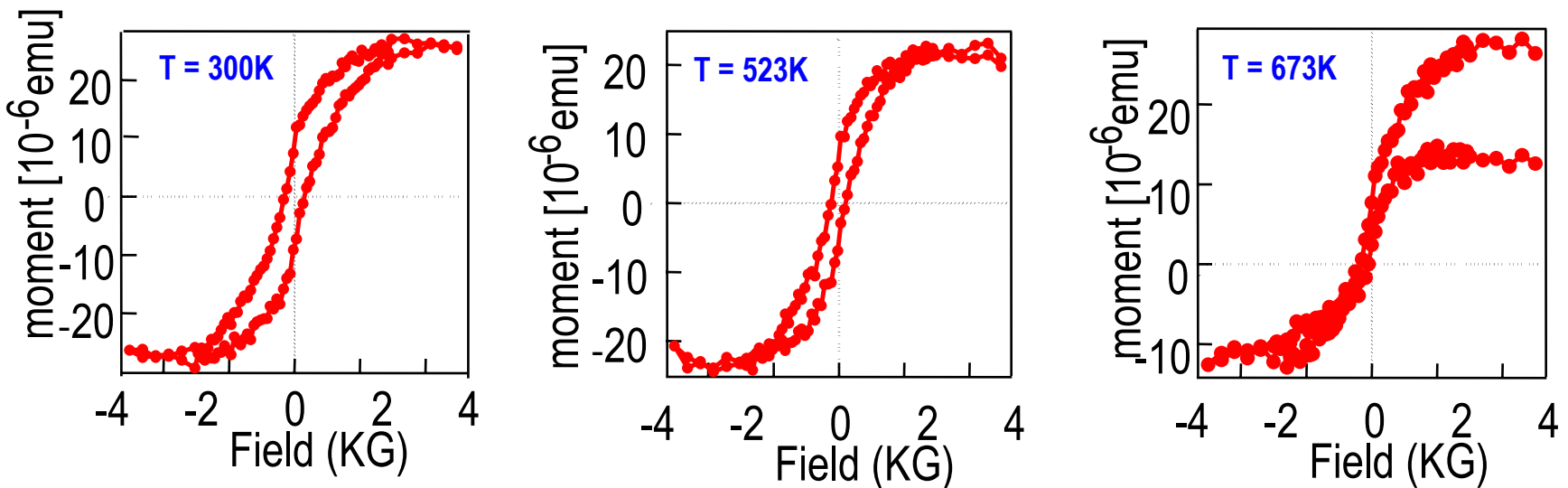
100 nm $\text{Co}_{0.02}\text{Ti}_{0.98}\text{O}_{1.98}/\text{SrTiO}_3(001)$ -- SQUID



- No reduction in magnetic moment up to 300K
- Curie temperature > 300K
- Highest Curie temperature for Mn-doped III-Vs = 110K

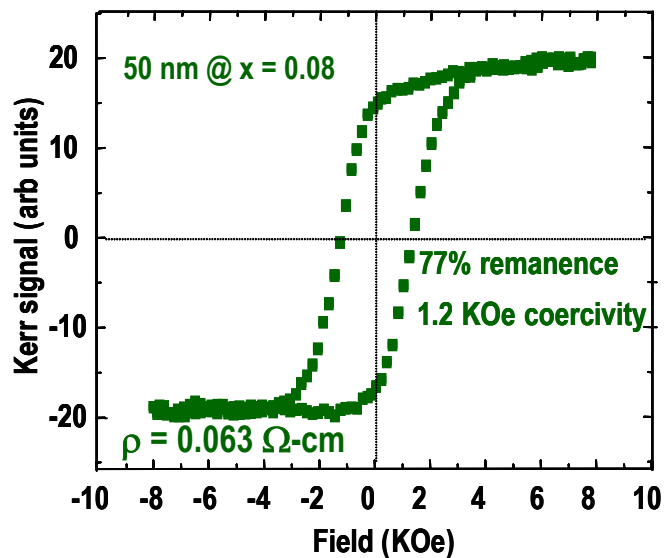
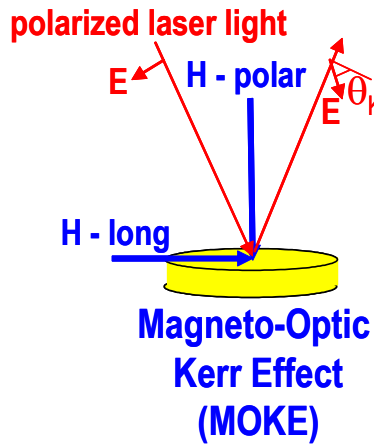
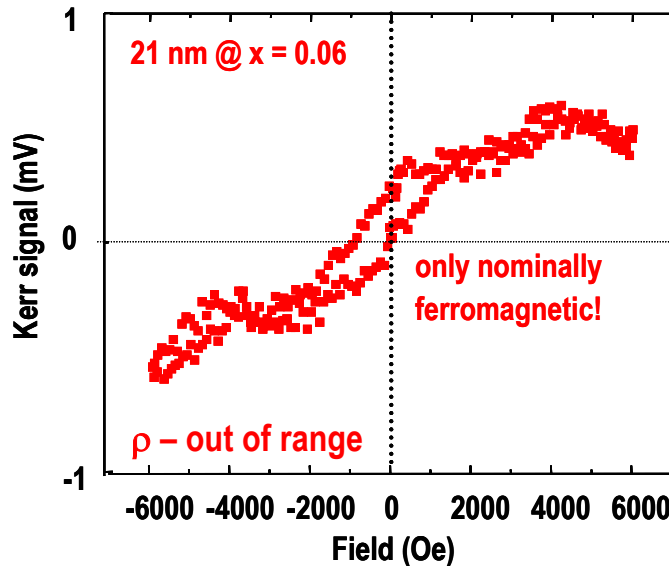
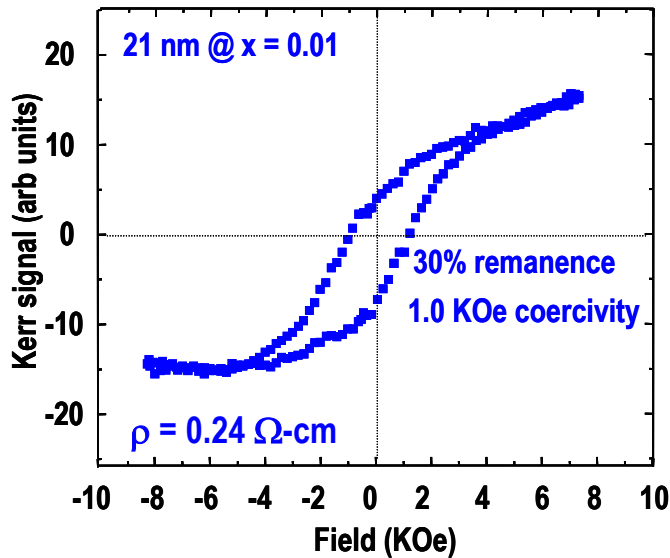
Magnetic Properties vs. Temperature - STO

VSM above room temperature in an Ar-purged cell



- Sample had to be cut from $1 \times 1 \text{ cm}^2$ square to 0.6 cm diameter circle for temperature dependent VSM above RT → damage → relatively poor RT loop
- Moment at 523K is ~20% lower than moment at RT, but still in tact
- Coercivity near zero at 673K , *but film is still magnetic!*
- Curie temperature > $\sim 500\text{K}$ (more precise experiments are in progress)

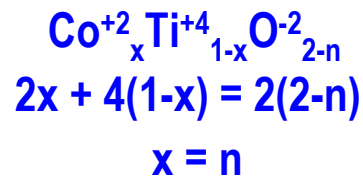
Relationship Between Magnetization and Conductivity – Single Crystal Films on LAO



- electron mediated exchange interaction!

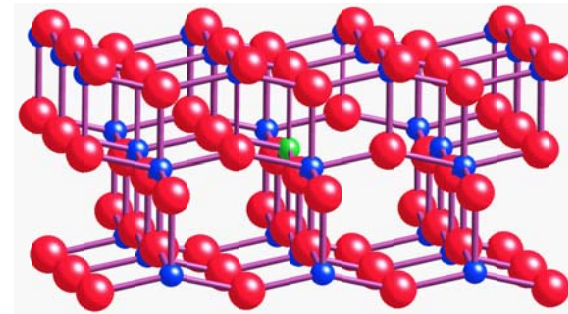
(Tentative) Relationship Between Electronic and Magnetic Properties in $\text{Co}_x\text{Ti}_{1-x}\text{O}_2$

- O vacancies accompanying Co substitution for Ti (required for charge neutrality)



O^{-2} vacancies \rightarrow no donor electrons

(explains why some films with lots of Co are not magnetic)



- The cause of n-type doping -- substitutional OH (anatase reduction by H_2 during growth ?)



One donor electron per OH

(H present in the films at $10^{19} - 10^{20} \text{ cm}^{-3}** \rightarrow$ same order of magnitude as electron density)

** ${}^{19}\text{F}({}^1\text{H}, \alpha\gamma){}^{16}\text{O}$ – resonance at 6.42 MeV. Resolution = 20 nm (FWHM = 40 keV). 20 nm sampling depth at 6.42 MeV. Greater depth penetration at higher energy \rightarrow 1-2 μm at 9.5 MeV.

Conclusions

- Epitaxial Co-doped anatase ($\text{Co}_x\text{Ti}_{1-x}\text{O}_{2-x}$ -- $x \leq \sim 0.1$) grown on SrTiO_3 and $\text{LaAlO}_3(001)$ by OPA-MBE. Best results on LAO ($\Delta a/a = -0.26\%$).
- $\text{Co}_x\text{Ti}_{1-x}\text{O}_{2-x}$ ferromagnetic at temperatures of $> 300\text{K}$. Moment = $\sim 1.2 - 1.4 \mu_B$ per Co at 300K. *Curie temperature is at least 500K*. Magnetic properties of MBE-grown material are significantly better than those for PLD-grown $\text{Co}_x\text{Ti}_{1-x}\text{O}_{2-x}$.
- Magnetic and structural properties depend critically on growth parameters
Best properties for films grown at slow growth rate ($\sim 0.01 \text{ nm/sec}$)
- Co substitutes for Ti, and is in the +2 formal oxidation state. Results in O^{2-} (uncharged) vacancies; 1 O^{2-} per substitutional Co^{+2} .
- Material is *n*-type (OH derived donors?) \rightarrow electron mediated exchange interaction. *Magnetization depends as much on conductivity as on Co content.*
- Potential epitaxial spin injector for *n*-Si ($\Delta a/a = -1.6\%$, $\sigma_{\text{Si}} \sim \sigma_{\text{ana}}$). $\text{Co}_x\text{Ti}_{1-x}\text{O}_{2-x}$ heteroepitaxy on Si(001) to start soon with M.A. Olmstead and D. Schmidt (UW – Physics)
- For more details, see APL 79, 3467 (2001) and Mat. Today, April (2002).